

1

Version dated: April 27, 2017

2 **So many genes, so little time: comments on**
3 **divergence-time estimation in the genomic era**

4 STEPHEN A. SMITH¹, AND JOSEPH W. BROWN^{1†}, JOSEPH F. WALKER^{1†}

5 ¹*Department of Ecology and Evolutionary Biology, University of Michigan, Ann Arbor, Michigan,*
6 *48109, USA*

7 [†]*Equal contribution*

8 **Corresponding author:** Stephen A. Smith, Ecology and Evolutionary Biology,
9 University of Michigan, Ann Arbor, Michigan, 48109, USA; E-mail: eebsmith@umich.edu.

10

ABSTRACT

- 11 1. Phylogenomic datasets have emerged as an important tool and have been used for
12 addressing questions involving evolutionary relationships, patterns of genome
13 structure, signatures of selection, and gene and genome duplications. Here, we
14 examine these data sources for their utility in the estimation of divergence-times.
15 Divergence-time estimation can be complicated by the heterogeneity of molecular
16 rates among lineages and through time. Despite the recent explosion of phylogenomic
17 data, it is still unclear what the distribution of gene- and lineage-specific rate
18 heterogeneity is over these genomic and transcriptomic datasets.
- 19 2. Here, we examine rate heterogeneity across genes and determine whether clock-like or
20 nearly clock-like genes are present in phylogenomic datasets that could be used to
21 reduce error in divergence-time estimation. We address these questions with six
22 published phylogenomic datasets including Birds, carnivorous Caryophyllales, broad
23 Caryophyllales, Millipedes, Hymenoptera, and Vitales. We introduce a simple and
24 fast method for identifying useful genes for constructing divergence-time estimates

25 and conduct exemplar Bayesian analyses under both clock and uncorrelated
26 log-normal (UCLN) models.

- 27 3. We used a “gene shopping” approach (implemented in `SortaDate`) to identify genes
28 with minimal conflict, lower root-to-tip variance, and discernible amounts of
29 molecular evolution. We find that every empirical dataset examined includes genes
30 with clock-like, or nearly clock-like, behavior. Many datasets have genes that are not
31 only clock-like, but also have reasonable evolutionary rates and are mostly
32 compatible with the species tree. We used these data to conduct basic
33 divergence-time analyses under strict clock and UCLN models. These exemplar
34 divergence-time analyses show overlap in age estimates when using either clock or
35 UCLN models, but with much larger credibility intervals for UCLN models.
- 36 4. We find that “gene shopping” can be productive and successful in finding gene regions
37 that minimize lineage-specific heterogeneity. By doing relatively simple assessments
38 of root-to-tip variance and bipartition conflict, we not only explore datasets more
39 thoroughly but also may estimate ages on phylogenies with lower error. We also
40 suggest the need to explore more detailed and informative approaches to determine fit
41 and deviation from a molecular clock, as existing approaches are exceedingly strict.

42 *Introduction*

43 Divergence-time estimation is a complicated, but often essential, step for many
44 phylogenetic analyses. The sources of error include the ambiguous nature of fossil
45 placement, model mis-specification (e.g., involving significant variation in the branchwise
46 and/or sitewise rates of evolution), uncertainty in the phylogenetic tree, topological
47 dissonance amongst gene trees due to incomplete lineage sorting, and complexity of the
48 model for the molecular clock (e.g., Smith *et al.* 2010; Dornburg *et al.* 2012; Parham *et al.*
49 2012; Heath and Moore 2014; Beaulieu *et al.* 2015; Kumar and Hedges 2016). While fossils
50 give the only available information for absolute age, their placement and age carry

51 uncertainty. Multiple fossil calibrations and complicated tree shape priors can interact to
52 further complicate molecular dating (Zhu *et al.* 2015; Heled and Drummond 2015; Rannala
53 2016; dos Reis 2016; Brown and Smith 2017). Rate variation is common among individual
54 branches of a phylogeny and can constitute extensive deviations from the molecular clock.
55 As a result, complex models have been developed to accommodate for these deviations
56 (Sanderson 2002; Drummond *et al.* 2006; Drummond and Suchard 2010). However, these
57 more parameter-rich models also carry with them significant uncertainty and can, when the
58 data deviate significantly from the model, lead to biased results (e.g., Worobey *et al.* 2014).
59 Despite these difficulties, researchers continue to use divergence-time estimates extensively
60 as they remain essential for many downstream evolutionary and comparative analyses.

61 Datasets based on thousands of genes from genomes and transcriptomes have
62 emerged as a major tool in addressing broad evolutionary questions including, but not
63 limited to, phylogenetic reconstruction, gene and genome duplication, and inference of
64 molecular evolutionary patterns and processes. And while these datasets have been used
65 for divergence-time estimation (e.g., Jarvis *et al.* 2014b; Prum *et al.* 2015), their overall
66 utility for divergence-time analyses has not been fully examined. In particular, it is unclear
67 whether within these enormous datasets there exist nearly clock-like gene regions that may
68 aid in producing lower error divergence-time estimates. While some authors of recent large
69 genomic analyses, such as Jarvis *et al.* (2014b), have suggested choosing clock-like genes, a
70 repeatable and fast procedure to identify these genes has not been explored for
71 phylogenomics and an examination of the frequency of these genes in empirical datasets
72 has not been conducted.

73 Researchers can take steps to ease sources of errors for divergence-time analyses. For
74 example, better use of fossils in temporal calibrations can dramatically improve estimations
75 (e.g., Parham *et al.* 2012; Ksepka *et al.* 2015), as does better accounting for rate variation
76 in the molecular models by improving model fit. Several relaxed clock models have been
77 introduced over the last few decades to accommodate rate heterogeneity because most data
78 do not conform to a strict clock. The most commonly used relaxed clock methods include

79 penalized likelihood (PL, Sanderson 2002) as implemented in `r8s` (Sanderson 2003) (and
80 more recently in `treePL` (Smith and O’Meara 2012)), and Bayesian uncorrelated rate
81 models (e.g., the uncorrelated lognormal (UCLN) model; Drummond *et al.* (2006)) as
82 implemented in `BEAST` (Drummond and Rambaut 2007) and `MrBayes` (Ronquist *et al.*
83 2012), although many other methods have been developed and new ones are continually
84 released (e.g., Takezaki *et al.* 1995; Thorne and Kishino 2002; Lartillot and Philippe 2004;
85 Britton *et al.* 2007; Lepage *et al.* 2007; Rannala and Yang 2007; Drummond and Suchard
86 2010; Tamura *et al.* 2012; Heath *et al.* 2014; Ronquist *et al.* 2016; Lartillot *et al.* 2016).
87 The diversity of techniques is matched with a variety of different inputs. For example, PL
88 implementations minimally require an estimated phylogram, calibration, smoothing
89 penalty value, and alignment size, while full Bayesian methods minimally require an
90 alignment and priors to be set for each parameter, including any fossil calibrations.

91 Bayesian methods that use relaxed clock models, such as those implemented in
92 `BEAST`, `MrBayes`, and `PhyloBayes` (Lartillot and Philippe 2004), simultaneously estimate
93 phylogenetic relationships and divergence times, and so may be preferred over other
94 approaches as Bayesian methods incorporate uncertainty more easily and explicitly.
95 However, the computational burden of these simultaneous reconstruction methods limit
96 their use to smaller datasets (i.e., excluding entire genomes and transcriptomes).
97 Fortunately, a prescient solution to this dilemma was proffered two decades ago with the
98 concept of “gene shopping” (Hedges *et al.* 1996; Kumar and Hedges 1998), wherein
99 available genes are filtered by how well they conform to a molecular clock. [A related
100 procedure, “taxon-shopping” (Takezaki *et al.* 1995; van Tuinen and Hedges 2001; van
101 Tuinen and Dyke 2004), prunes taxa from an alignment until the dataset no longer rejects
102 a molecular clock test. We do not consider this approach here.]. Using “gene shopping”, it
103 should be possible to reduce larger datasets to alignments that are capable of being
104 analyzed by Bayesian methods. However, despite the having been available for decades,
105 “gene shopping” has not been widely applicable before the recent development of
106 next-generation sequencing techniques because of the relatively small number of genes

107 available for any single clade (outside of model organisms). However, as genomic and
108 transcriptomic datasets have become more readily available, “gene shopping” holds
109 tremendous promise as a tool for inferring phylogenetic timescales. Nevertheless, the utility
110 of these large genomic datasets for divergence-time estimation and the distribution of
111 lineage-specific rate heterogeneity has yet to be fully explored.

112 Next generation sequencing techniques have dramatically increased the number of
113 gene regions available for phylogenetic analysis. This has stimulated research into questions
114 that are specifically pertinent to datasets with hundreds or thousands of genes. What is
115 the best method for reconstructing the species tree (e.g., Gatesy and Springer 2014;
116 Mirarab *et al.* 2014; Roch and Warnow 2015)? How many genes support the dominant
117 species tree signal (e.g., Salichos *et al.* 2014; Smith *et al.* 2015)? Genomic datasets also
118 allow us to examine the extent of molecular rate variation in genes, genomes, and lineages.
119 For example, Yang *et al.* (2015) explored the distribution of lineage-specific rate
120 heterogeneity throughout transcriptomes of the plant clade Caryophyllales as it relates to
121 life history. Jarvis *et al.* (2014b), analyzing a genomic dataset of birds, explored rate
122 heterogeneity and selection as it relates to errors in phylogeny reconstruction in a genomic
123 dataset of birds. Recently, the clock-likeness of phylogenomic datasets has come of interest
124 to the community. For example, Doyle *et al.* (2015) attempt to identify strictly clock-like
125 genes in order to avoid long branch attraction artifacts in phylogenetic inference. Jarvis
126 *et al.* (2014b) recently filtered gene regions by inferred mean coefficient of rate variation (a
127 measure of clock-likeness) from full Bayesian analyses of each gene, to identify “clock-like”
128 genes explicitly for divergence-time estimation. However, while these authors have
129 conducted filtering analysis on their genomic data, a thorough examination of
130 lineage-specific rate heterogeneity across clades for divergence-time estimation has not been
131 conducted. Nevertheless, the availability of full genomes and transcriptomes makes
132 identifying genes with lower rate variation possible and so are more suitable for
133 divergence-time estimation.

134 Here we present one means of utilizing genomic data for estimating divergence time

135 by introducing a simple sorting procedure to identify informative (i.e., does not conflict
136 strongly with an existing species tree hypothesis, and possesses appreciable tree length)
137 and nearly clock-like (i.e., low variance) genes. Genes that fit these criteria may simplify a
138 convenient divergence-time estimation for large datasets as methods such as clock
139 partitioning are difficult when dealing with dozens, hundreds, or even thousands of genes
140 Duchêne *et al.* (2013). Additionally, this procedure can be used to examine the overall
141 distribution of evolution, rate heterogeneity, bipartition concordance, and potential utility
142 of genes for divergence-time analysis. It is assumed that a researcher will possess a
143 phylogenetic hypothesis of their taxon, inferred (in some manner) from the entire corpus of
144 available genetic sequences. Thus, the procedure described here is aimed at dating an
145 existing phylogenetic hypothesis using a subset of the genetic data. The procedure holds
146 promise that, while various relaxed clock models are available (conducive to
147 accommodating different forms of rate heterogeneity), data that do not require extensive
148 rate modelling will enable fast, accurate, and precise divergence time estimates (see also To
149 *et al.* 2015). Finally, we examine six genomic and transcriptomic datasets across animals
150 and plants and with different temporal and taxonomic scopes to examine the extent of
151 lineage-specific rate heterogeneity. We investigate the distribution of variation in the
152 branchwise rates of evolution across thousands of genes to understand whether these new
153 genomic resources may improve divergence-time estimation by allowing for simpler models
154 of molecular evolution.

155 *Materials and Methods*

156 *Availability of procedures.*— The analyses performed below can be conducted using the
157 **SortaDate** package (with source code and instructions available at
158 <https://github.com/FePhyFoFum/sortadate>). This package is written in Python and
159 available as an Open Source set of procedures. In some cases, external programs are used
160 (e.g., those found in the **Phyx** package (Brown *et al.* 2017)) that are also Open Source and
161 freely available.

162 *Dataset processing.*— We used six published datasets to examine rate heterogeneity: Birds
163 (BIR, Jarvis *et al.* 2014b), carnivorous Caryophyllales (CAR, Walker *et al.* 2017), the
164 broader Caryophyllales (CARY, Yang *et al.* 2015), Vitales (VIT, Wen *et al.* 2013),
165 Hymenoptera (HYM, Johnson *et al.* 2013), and Millipedes (MIL, Brewer and Bond 2013).
166 The range in datasets spans different taxonomic groups, datasets sizes (e.g., CAR vs
167 CARY), and age (e.g., from hundreds of millions of years to within the last hundred million
168 years). Where possible, we used orthologs that were identified using the Maximum
169 Inclusion method of Yang and Smith (2015). This was the case with every dataset but BIR
170 for which we used the exon alignments available online (Jarvis *et al.* 2014a;
171 <http://gigadb.org/dataset/101041>). For each ortholog, we have an estimated gene tree,
172 based on maximum likelihood (ML) analyses, and alignments, from the original studies.
173 Gene trees, regardless of the source of orthologs, were then rooted and SH-like tests were
174 performed to assess confidence in edges (Anisimova and Gascuel 2006). We note that gene
175 tree rooting is a requirement of the SortaDate procedure. This is typically performed using
176 outgroups.

177 *Gene tree analyses.*— Because deviation from the clock is empirically manifest in a
178 phylogram as variation in root-to-tip length among tips within a tree, we measured the
179 variance of root-to-tip lengths for each tree. This was performed on each rooted ortholog,
180 for which outgroups were removed, with the `pxlstr` program of `Phyx` package (Brown
181 *et al.* 2017). We performed the standard clock test for each ortholog (Muse and Weir
182 1992), with outgroup removed, using `PAUP*` v4.0a151 (Swofford 2001) by calculating the
183 ML score for a gene both with and without assuming a clock, and then performing a
184 likelihood ratio test. In addition to assessing the clock-likeness of genes, we also compared
185 gene tree topologies to the corresponding published species tree topology. Branch lengths
186 were not available for some species trees. To compare the individual gene trees to their
187 corresponding species trees, we conducted bipartition comparison analyses on each gene
188 tree using `pxbp` from the `Phyx` package (procedure described in Smith *et al.* 2015).

189 *Simulations.*— We conducted simulations to examine expectations of rate variation given

190 clock-like, noisy clock-like, and uncorrelated lognormal data. We first generated simulated
191 clock-like data using `Indelible` v1.03 (Fletcher and Yang 2009) using the WAG model
192 with 500 characters for amino acid datasets, and JC with 1500 characters for nucleotide
193 datasets, on each of the empirical species tree topologies. For these data simulations,
194 because the species tree often had no branch lengths available, node heights were first
195 simulated randomly using `Indelible` and then the tree was rescaled to a height of 0.25,
196 0.5, or 0.75. We used the trees generated by `Indelible` to further simulate 100 noisy clock
197 (rate=1.0, noise=0.25, and rate=1.0, noise=0.75) and uncorrelated lognormal (UCLN)
198 trees (mean.log=-0.5, stdev.log=0.5, and mean.log=-0.5, stdev.log=1.0) using `NELSI` v0.21
199 (Ho *et al.* 2015). We note the ‘noise’ in `NELSI` corresponds to the standard deviation of a
200 normal distribution with mean = 0. For the noisy clock, branch-specific rates are a sum of
201 the global rate (here, 1.0) and a draw from this normal distribution. The simulations with
202 noise=0.75 thus are only loosely clock-like, and serve as a comparison between the more
203 clock-like (noise=0.25) and UCLN analyses. We used `RAxML` v8.2.3 (Stamatakis 2014) to
204 reconstruct each of these datasets. For each simulation, we examined the rate variation and
205 the root-to-tip length variation on the reconstructed phylograms.

206 While the focus of this study is not the performance of divergence-time estimation
207 methods, we still wanted to examine an exemplar from the simulations to ascertain the
208 variation in the results given different clock models. We used one random realization of
209 node heights as simulated from the `Indelible` analyses as mentioned above to generate
210 two datasets with `NELSI`. One dataset had three genes generated from a clock rate of 1 and
211 noise at 0.25, and the other dataset had three genes generated from a UCLN model and
212 mean.log at -0.5 and sd.log=1. As above, each amino acid gene consisted of 500 residues,
213 while DNA genes consisted of 1500 nucleotides. For each simulation, all three genes shared
214 a common topology (but with different edge lengths, as our filtering procedure involves a
215 single focal topology). For both the noisy clock-like and UCLN datasets, we conducted
216 `BEAST` analyses with both a clock model and a UCLN model. A birth-death tree prior was
217 used as the prior for all node heights, and runs were conducted for 10 million generations

218 with the first 10% discarded as burnin. Results were summarized using `treeannotator`
219 from the BEAST package. Median node heights as well as 95% HPD node heights were
220 compared between the simulated datasets and the tree used to generate these datasets.

221 *Sorting and dating analyses on real data.*— In addition to these analyses on simulated
222 datasets, we conducted divergence-time analyses on a subset of the empirical datasets.
223 Because these datasets consist of hundreds to thousands of genes, we developed a sorting
224 procedure intended to mimic that which would be performed as a “gene shopping”
225 analysis. The sorting procedure relies on the root-to-tip variance statistic, bipartition
226 calculation to determine the similarity to the species tree, and total treelength. We sorted
227 first by the similarity to the species tree, then root-to-tip variance, and finally treelength.
228 For these examples we limited the results to the top three genes reported from the sorting
229 procedure, although for empirical analyses one should choose the number of genes by
230 carefully examining the filtering results. Because we filtered for genes that were consistent
231 with the species tree, these genes were then concatenated and the topology was fixed to be
232 consistent with the species tree. We applied individual substitution models to each gene
233 within a data set. However, given that the genes were filtered both to match the species
234 tree and for clock-likeness, we modelled all genes with a single molecular clock (albeit with
235 gene-specific relative rates). For each of these datasets, we conducted two BEAST analyses,
236 one assuming a strict clock and the other assuming a UCLN model. Because specific dates
237 were not the focus of this examination, the birth-death tree prior was used instead of fossil
238 priors for nodes. The analyses were run in duplicate for 10 million generations (the BIR
239 and CARY UCLN analyses took longer to reach convergence, and so was run for 50 million
240 generations) with the first 10% discarded as burnin. Replicate MCMC logs were
241 concatenated while removing burnin using the `pxlog` program from the `Phyx` package, and
242 finally summarized using `treeannotator` as above. Median node heights and 95% HPD
243 node heights were compared between the clock and UCLN runs as the node heights on the
244 true phylogeny are unknown.

245

Results and Discussion

246 A fundamental question for each of the empirical datasets is: are there clock-like gene
247 regions present within the genome? Results were varied, from 0.4% of genes passing the
248 clock test for the VIT dataset to 17% for the MIL dataset (see Table 1). These results are
249 not surprising, as even with clock-like genes it is expected that stochastic differences will
250 accumulate with both increased sampling (i.e., more edges) and older trees (i.e., longer
251 edges). As for size, the CAR dataset has 7 taxa that are not included in the CARY dataset
252 but otherwise overlaps partially and has far fewer taxa in total. The CARY dataset, in
253 addition to being much larger, also contains known shifts in life history (Yang *et al.* 2015).
254 These differences may account for the variation between these two datasets. As for clade
255 age, HYM and MIL are significantly older than the other datasets, which may account for
256 their rate variation. Nevertheless, each dataset indeed had at least a few orthologs that
257 passed a strict clock test even if these orthologs were in the small minority.

258 Because passing a clock test does not necessarily indicate that the gene would be
259 good for phylogenetic reconstruction, we also measured treelength and root-to-tip variance
260 for each ortholog (see Figures 2-3). Clock tests are stringent in their need to conform to
261 the clock (see below) and so by examining the root-to-tip variation and lineage-specific
262 variation, we are more directly examining the deviation from ultrametricity. Although this
263 is primarily descriptive and does not include a formal test, this provides an easily
264 interpretable characterization of rate variation. We found that the datasets vary
265 dramatically with no discernible general pattern for both root-to-tip variance and
266 treelength. For example, the BIR dataset demonstrates very little molecular evolution as
267 demonstrated by the short treelengths. For this dataset, we analyzed nucleotides (rather
268 than amino acids) to maximize treelengths as Jarvis *et al.* (2014b) demonstrated low rates
269 of evolution, especially deep in the phylogeny. However, the inferred rates of evolution (as
270 determined by overall tree length) were still low. Given the difficulty in resolving the avian
271 phylogeny, this pattern is perhaps to be expected (Jarvis *et al.* 2014b). This same pattern
272 is present in the VIT dataset, though this was not explored as thoroughly in the original

273 publication. Both the CAR and CARY datasets show a pattern of increasing variance with
274 greater treelength (Figures 2). This contrasts with the HYM and MIL datasets that are
275 clock-like even with longer treelengths (Figure 3). Lineage-specific rate variation in each
276 dataset was idiosyncratic with most extreme variation in the outgroups. While outgroups
277 were excluded for clock tests and in determining root-to-tip variance for “gene shopping”,
278 we allowed outgroups to remain for lineage-specific rate variation analyses as in the right
279 handed plots of Figure 3. The VIT dataset was an exception with several lineages other
280 than the outgroup having high rates. In each dataset, there were genes that fell within the
281 distribution of simulated trees that are clock-like or clock-like with low noise.

282 One potential benefit of identifying orthologs with lower lineage-specific rate
283 variation within phylogenomic datasets is to use these, or a subset of these, orthologs to
284 conduct divergence-time analyses. The hope is that by using clock-like genes, we may
285 overcome or lessen the impact of lineage-specific rate variation on the error of divergence
286 time analyses. The non-identifiability of rates and dates (e.g., longer branch lengths may
287 be the result of a long time or fast evolution) is exacerbated by lineage-specific rate
288 heterogeneity. We used a subset of orthologs to conduct divergence time analyses and we
289 implemented a sorting procedure (packed in `SortaDate`) to (i) filter the genes that best
290 reflect the species tree (i.e., higher bipartition concordance with the species tree), (ii) have
291 lower root-to-tip variance (i.e., most clock-like), and discernible amounts of molecular
292 evolution (i.e., greater tree length; Figure 1). For each empirical dataset, we generated
293 such an alignment (see Table 2). The genes that were filtered and used for divergence-time
294 analyses for the BIR, CARY, VIT, and HYM datasets rejected the clock. The genes for the
295 CAR and MIL datasets either didn’t or weakly rejected the clock. Resulting HPD trees
296 were rescaled so that the root heights were equivalent to allow for easier comparisons
297 between datasets. Typically, fossil placements would be used for scaling but because these
298 are not intended to be runs for future use, we eliminated fossil placements as one source of
299 variation. We found rough correspondence of node heights between the clock and UCLN
300 analyses, especially for the four smallest datasets (see Figure 4). The UCLN analyses, as

301 expected, had far greater variance in the 95% HPDs for node ages. We found the greatest
302 differences in the larger BIR and CARY datasets (see Table 3) where there are major
303 differences in tree heights. This may reflect the size of the dataset or the underlying rate
304 variation in the datasets. In general, strict clock estimates resulted in younger median node
305 ages than analogous UCLN estimates, as well as younger maximum and older minimum
306 95% HPD values (see Table 3). The coefficient of rate variation statistics (an measure of
307 clock-likeness) for UCLN runs ranged from the lowest mean values of 0.2358
308 (stErr=0.0347) in HYM to the highest of 1.2464 (stErr=0.1135) in CARY.

309 As is always the problem with real datasets, the true divergence-times are unknown.
310 So we conducted exemplar analyses. For each empirical dataset, we simulated data for
311 three genes under both noisy clock and UCLN models to examine the variation in the
312 resulting divergence-time analyses where the true dates were known. For these simulated
313 datasets, a strict clock was rejected in each case, including those datasets that were
314 simulated under a clock with noise. We compared the resulting node heights from the
315 divergence time analyses under clock and UCLN models with the tree used for simulation
316 (see Tables 4-5 and Figure 5). For the datasets generated under a noisy clock model, more
317 of the true node heights were found in the 95% HPD interval when using the UCLN model
318 for inference than the strict clock model for inference. However, the precision as measured
319 by the total width of the 95% HPD interval for the UCLN runs were much lower than the
320 clock runs (see Tables 4-5). Those nodes that were not within the interval of the 95% HPD
321 when using the strict clock model for reconstruction, were close to the true value. So, while
322 fewer true node ages were contained in the strict clock HPDs, the overall error rate was
323 lower. For example, in the CARY dataset, while fewer nodes in the clock estimate were
324 found to be within the interval (52 vs 67 for the UCLN), the distance of the interval from
325 the estimate was lower for the clock dataset for both the high and low value for the 95%
326 HPD. Stated another way, the UCLN intervals were large enough that the true age was
327 often included, but this was at the cost of far lower precision. Because of this error relative
328 to the strict clock, the UCLN perhaps should not be the preferred model, especially if the

355

Data availability

356 All unpublished analyses and datasets are available through Data Dryad (#XXXXXX).

357 Associated scripts related to the method are available on GitHub at

358 <https://github.com/FePhyFoFum/sortadate>.

359

Author contributions

360 SAS, JWB, and JFW conceived of the project. SAS, JFW, and JWB analyzed the data.

361 SAS, JWB, and JFW wrote the manuscript.

*

362

363 References

364 Anisimova, M. and Gascuel, O. 2006. Approximate likelihood-ratio test for branches: A
365 fast, accurate, and powerful alternative. *Systematic Biology*, 55(4): 539–552.

366 Beaulieu, J. M., O’Meara, B. C., Crane, P., and Donoghue, M. J. 2015. Heterogeneous
367 rates of molecular evolution and diversification could explain the triassic age estimate for
368 angiosperms. *Systematic Biology*, 64(5): 869–878.

369 Brewer, M. S. and Bond, J. E. 2013. Ordinal-level phylogenomics of the arthropod class
370 diplopoda (millipedes) based on an analysis of 221 nuclear protein-coding loci generated
371 using next-generation sequence analyses. *PLoS ONE*, 8(11): e79935.

372 Britton, T., Anderson, C. L., Jacquet, D., Lundqvist, S., and Bremer, K. 2007. Estimating
373 divergence times in large phylogenetic trees. *Systematic Biology*, 56(5): 741–752.

374 Brown, J. W. and Smith, S. A. 2017. The past sure is tense: On interpreting phylogenetic
375 divergence time estimates. *bioRxiv*, 113720.

376 Brown, J. W., Walker, J. F., and Smith, S. A. 2017. phyx: Phylogenetic tools for Unix.
377 *Bioinformatics*. doi: 10.1093/bioinformatics/btx063.

378 Dornburg, A., Brandley, M. C., McGowen, M. R., and Near, T. J. 2012. Relaxed clocks
379 and inferences of heterogeneous patterns of nucleotide substitution and divergence time
380 estimates across whales and dolphins (mammalia: Cetacea). *Molecular Biology and
381 Evolution*, 29(2): 721–736.

382 dos Reis, M. 2016. Notes on the birth–death prior with fossil calibrations for Bayesian
383 estimation of species divergence times. *Philosophical Transactions of the Royal Society of
384 London B: Biological Sciences*, 371(1699): 20150128.

- 385 Doyle, V. P., Young, R. E., Naylor, G. J., and Brown, J. M. 2015. Can we identify genes
386 with increased phylogenetic reliability? *Systematic Biology*, 64(5): 824–837.
- 387 Drummond, A. J. and Rambaut, A. 2007. BEAST: Bayesian evolutionary analysis by
388 sampling trees. *BMC Evolutionary Biology*, 7(1): 214.
- 389 Drummond, A. J. and Suchard, M. A. 2010. Bayesian random local clocks, or one rate to
390 rule them all. *BMC Biology*, 8(1): 114.
- 391 Drummond, A. J., Ho, S. Y., Phillips, M. J., Rambaut, A., *et al.* 2006. Relaxed
392 phylogenetics and dating with confidence. *PLoS Biology*, 4(5): 699.
- 393 Duchêne, S., Molak, M., and Ho, S. Y. 2013. Clockstar: choosing the number of
394 relaxed-clock models in molecular phylogenetic analysis. *Bioinformatics*, page btt665.
- 395 Fletcher, W. and Yang, Z. 2009. INDELible: a flexible simulator of biological sequence
396 evolution. *Molecular Biology and Evolution*, 26(8): 1879–1888.
- 397 Gatesy, J. and Springer, M. S. 2014. Phylogenetic analysis at deep timescales: Unreliable
398 gene trees, bypassed hidden support, and the coalescence/concatalescence conundrum.
399 *Molecular Phylogenetics and Evolution*, 80: 231–266.
- 400 Heath, T. A. and Moore, B. R. 2014. Bayesian inference of species divergence times. In
401 M.-H. Chen, L. Kuo, and P. O. Lewis, editors, *Bayesian Phylogenetics: Methods*
402 *Algorithms, and Applications*, chapter 13, pages 277–318. CRC Press, Boca Raton,
403 Florida.
- 404 Heath, T. A., Huelsenbeck, J. P., and Stadler, T. 2014. The fossilized birth–death process
405 for coherent calibration of divergence-time estimates. *Proceedings of the National*
406 *Academy of Sciences*, 111(29): E2957–E2966.
- 407 Hedges, S. B., Parker, P. H., Sibley, C. G., and Kumar, S. 1996. Continental breakup and
408 the ordinal diversification of birds and mammals. *Nature*, 381(6579): 226–229.

- 409 Heled, J. and Drummond, A. J. 2015. Calibrated birth–death phylogenetic time-tree priors
410 for Bayesian inference. *Systematic Biology*, 64(3): 369–383.
- 411 Ho, S. Y. W., Duchêne, S., and Duchêne, D. 2015. Simulating and detecting
412 autocorrelation of molecular evolutionary rates among lineages. *Molecular Ecology*
413 *Resources*, 15(4): 688–696.
- 414 Jarvis, E., Mirarab, S., Aberer, A., Houde, P., Li, C., Ho, S., Faircloth, B., Nabholz, B.,
415 Howard, J., Suh, A., Weber, C., Fonseca, R., Alfaro-Nunez, A., Narula, N., Liu, L., Burt,
416 D., Ellegren, H., Edwards, S., Stamatakis, A., Mindell, D., Cracraft, J., Braun, E.,
417 Warnow, T., Jun, W., Gilbert, M., and Zhang, G. 2014a. Phylogenomic analyses data of
418 the avian phylogenomics project. *GigaScience*, 4(1): 4.
- 419 Jarvis, E. D., Mirarab, S., Aberer, A. J., Li, B., Houde, P., Li, C., Ho, S. Y. W., Faircloth,
420 B. C., Nabholz, B., Howard, J. T., Suh, A., Weber, C. C., da Fonseca, R. R., Li, J.,
421 Zhang, F., Li, H., Zhou, L., Narula, N., Liu, L., Ganapathy, G., Boussau, B., Bayzid,
422 M. S., Zavidovych, V., Subramanian, S., Gabaldón, T., Capella-Gutiérrez, S.,
423 Huerta-Cepas, J., Rekepalli, B., Munch, K., Schierup, M., Lindow, B., Warren, W. C.,
424 Ray, D., Green, R. E., Bruford, M. W., Zhan, X., Dixon, A., Li, S., Li, N., Huang, Y.,
425 Derryberry, E. P., Bertelsen, M. F., Sheldon, F. H., Brumfield, R. T., Mello, C. V.,
426 Lovell, P. V., Wirthlin, M., Schneider, M. P. C., Prosdocimi, F., Samaniego, J. A.,
427 Velazquez, A. M. V., Alfaro-Núñez, A., Campos, P. F., Petersen, B., Sicheritz-Ponten,
428 T., Pas, A., Bailey, T., Scofield, P., Bunce, M., Lambert, D. M., Zhou, Q., Perelman, P.,
429 Driskell, A. C., Shapiro, B., Xiong, Z., Zeng, Y., Liu, S., Li, Z., Liu, B., Wu, K., Xiao, J.,
430 Yinqi, X., Zheng, Q., Zhang, Y., Yang, H., Wang, J., Smeds, L., Rheindt, F. E., Braun,
431 M., Fjeldsa, J., Orlando, L., Barker, F. K., Jønsson, K. A., Johnson, W., Koepfli, K.-P.,
432 O’Brien, S., Haussler, D., Ryder, O. A., Rahbek, C., Willerslev, E., Graves, G. R.,
433 Glenn, T. C., McCormack, J., Burt, D., Ellegren, H., Alström, P., Edwards, S. V.,
434 Stamatakis, A., Mindell, D. P., Cracraft, J., Braun, E. L., Warnow, T., Jun, W., Gilbert,

- 435 M. T. P., and Zhang, G. 2014b. Whole-genome analyses resolve early branches in the
436 tree of life of modern birds. *Science*, 346(6215): 1320–1331.
- 437 Johnson, B. R., Borowiec, M. L., Chiu, J. C., Lee, E. K., Atallah, J., and Ward, P. S. 2013.
438 Phylogenomics resolves evolutionary relationships among ants, bees, and wasps. *Current*
439 *Biology*, 23(20): 2058–2062.
- 440 Ksepka, D. T., Parham, J. F., Allman, J. F., Benton, M. J., Carrano, M. T., Cranston,
441 K. A., Donoghue, P. C. J., Head, J. J., Hermsen, E. J., Irmis, R. B., Joyce, W. G., Kohli,
442 M., Lamm, K. D., Leehr, D., Patané, J. L., Polly, P. D., Phillips, M. J., Smith, N. A.,
443 Smith, N. D., Van Tuinen, M., Ware, J. L., and Warnock, R. C. M. 2015. The fossil
444 calibration database—a new resource for divergence dating. *Systematic Biology*, 64(5):
445 853–859.
- 446 Kumar, S. and Hedges, S. B. 1998. A molecular timescale for vertebrate evolution. *Nature*,
447 392(6679): 917–920.
- 448 Kumar, S. and Hedges, S. B. 2016. Advances in time estimation methods for molecular
449 data. *Molecular Biology and Evolution*, 33(4): 863–869.
- 450 Lartillot, N. and Philippe, H. 2004. A Bayesian mixture model for across-site
451 heterogeneities in the amino-acid replacement process. *Molecular Biology and Evolution*,
452 21(6): 1095–1109.
- 453 Lartillot, N., Phillips, M. J., and Ronquist, F. 2016. A mixed relaxed clock model.
454 *Philosophical Transactions of the Royal Society of London B: Biological Sciences*,
455 371(1699).
- 456 Lepage, T., Bryant, D., Philippe, H., and Lartillot, N. 2007. A general comparison of
457 relaxed molecular clock models. *Molecular Biology and Evolution*, 24(12): 2669–2680.
- 458 Mirarab, S., Bayzid, M. S., Boussau, B., and Warnow, T. 2014. Statistical binning enables
459 an accurate coalescent-based estimation of the avian tree. *Science*, 346(6215): 1250463.

- 460 Muse, S. and Weir, B. S. 1992. Testing for equality of evolutionary rates. *Genetics*, 132(1):
461 269–276.
- 462 Parham, J. F., Donoghue, P. C. J., Bell, C. J., Calway, T. D., Head, J. J., Holroyd, P. A.,
463 Inoue, J. G., Irmis, R. B., Joyce, W. G., Ksepka, D. T., Patané, J. S. L., Smith, N. D.,
464 Tarver, J. E., van Tuinen, M., Yang, Z., Angielczyk, K. D., Greenwood, J. M., Hipsley,
465 C. A., Jacobs, L., Makovicky, P. J., Müller, J., Smith, K. T., Theodor, J. M., Warnock,
466 R. C. M., and Benton, M. J. 2012. Best practices for justifying fossil calibrations.
467 *Systematic Biology*, 61(2): 346–359.
- 468 Prum, R. O., Berv, J. S., Dornburg, A., Field, D. J., Townsend, J. P., Lemmon, E. M., and
469 Lemmon, A. R. 2015. A comprehensive phylogeny of birds (Aves) using targeted
470 next-generation DNA sequencing. *Nature*, 526(7574): 569–573.
- 471 Rannala, B. 2016. Conceptual issues in Bayesian divergence time estimation. *Philosophical*
472 *Transactions of the Royal Society of London B: Biological Sciences*, 371(1699): 20150134.
- 473 Rannala, B. and Yang, Z. 2007. Inferring speciation times under an episodic molecular
474 clock. *Systematic Biology*, 56(3): 453–466.
- 475 Roch, S. and Warnow, T. 2015. On the robustness to gene tree estimation error (or lack
476 thereof) of coalescent-based species tree methods. *Systematic Biology*, 64(4): 663–676.
- 477 Ronquist, F., Teslenko, M., Van Der Mark, P., Ayres, D. L., Darling, A., Höhna, S.,
478 Larget, B., Liu, L., Suchard, M. A., and Huelsenbeck, J. P. 2012. MrBayes 3.2: efficient
479 Bayesian phylogenetic inference and model choice across a large model space. *Systematic*
480 *Biology*, 61(3): 539–542.
- 481 Ronquist, F., Lartillot, N., and Phillips, M. J. 2016. Closing the gap between rocks and
482 clocks using total-evidence dating. *Philosophical Transactions of the Royal Society of*
483 *London B: Biological Sciences*, 371(1699): 20150136.

- 484 Salichos, L., Stamatakis, A., and Rokas, A. 2014. Novel information theory-based measures
485 for quantifying incongruence among phylogenetic trees. *Molecular Biology and*
486 *Evolution*, 31(5): 1261–1271.
- 487 Sanderson, M. J. 2002. Estimating absolute rates of molecular evolution and divergence
488 times: a penalized likelihood approach. *Molecular Biology and Evolution*, 19(1): 101–109.
- 489 Sanderson, M. J. 2003. r8s: inferring absolute rates of molecular evolution and divergence
490 times in the absence of a molecular clock. *Bioinformatics*, 19(2): 301–302.
- 491 Smith, S. A. and O’Meara, B. C. 2012. treePL: divergence time estimation using penalized
492 likelihood for large phylogenies. *Bioinformatics*, 28(20): 2689–2690.
- 493 Smith, S. A., Beaulieu, J. M., and Donoghue, M. J. 2010. An uncorrelated relaxed-clock
494 analysis suggests an earlier origin for flowering plants. *Proceedings of the National*
495 *Academy of Sciences*, 107(13): 5897–5902.
- 496 Smith, S. A., Moore, M. J., Brown, J. W., and Yang, Y. 2015. Analysis of phylogenomic
497 datasets reveals conflict, concordance, and gene duplications with examples from animals
498 and plants. *BMC Evolutionary Biology*, 15(1): 150.
- 499 Stamatakis, A. 2014. RAxML version 8: a tool for phylogenetic analysis and post-analysis
500 of large phylogenies. *Bioinformatics*, 30(9): 1312–1313.
- 501 Swofford, D. L. 2001. PAUP*: Phylogenetic Analysis Using Parsimony (* and other
502 methods) 4.0.b5.
- 503 Takezaki, N., Rzhetsky, A., and Nei, M. 1995. Phylogenetic test of the molecular clock and
504 linearized trees. *Molecular Biology and Evolution*, 12(5): 823–833.
- 505 Tamura, K., Battistuzzi, F. U., Billig-Ross, P., Murillo, O., Filipowski, A., and Kumar, S.
506 2012. Estimating divergence times in large molecular phylogenies. *Proceedings of the*
507 *National Academy of Sciences*, 109(47): 19333–19338.

- 508 Thorne, J. L. and Kishino, H. 2002. Divergence time and evolutionary rate estimation with
509 multilocus data. *Systematic Biology*, 51(5): 689–702.
- 510 To, T.-H., Jung, M., Lycett, S., and Gascuel, O. 2015. Fast dating using least-squares
511 criteria and algorithms. *Systematic Biology*, 65(1): 82–97.
- 512 van Tuinen, M. and Dyke, G. J. 2004. Calibration of galliform molecular clocks using
513 multiple fossils and genetic partitions. *Molecular Phylogenetics and Evolution*, 30(1):
514 74–86.
- 515 van Tuinen, M. and Hedges, S. B. 2001. Calibration of avian molecular clocks. *Molecular
516 Biology and Evolution*, 18(2): 206–213.
- 517 Walker, J. F., Yang, Y., Moore, M. J., Mikenas, J., Brockington, S. F., Timoneda, A., and
518 Smith, S. A. 2017. Widespread paleopolyploidy, gene tree conflict and recalcitrant
519 relationships among the carnivorous caryophyllales. *bioRxiv*, 115741.
- 520 Wen, J., Xiong, Z., Nie, Z.-L., Mao, L., Zhu, Y., Kan, X.-Z., Ickert-Bond, S. M., Gerrath,
521 J., Zimmer, E. A., and Fang, X.-D. 2013. Transcriptome sequences resolve deep
522 relationships of the grape family. *PLoS ONE*, 8(9): e74394.
- 523 Worobey, M., Han, G.-Z., and Rambaut, A. 2014. A synchronized global sweep of the
524 internal genes of modern avian influenza virus. *Nature*, 508(7495): 254–257.
- 525 Yang, Y., Moore, M. J., Brockington, S. F., Soltis, D. E., Wong, G. K.-S., Carpenter, E. J.,
526 Zhang, Y., Chen, L., Yan, Z., Xie, Y., Sage, R. F., Covshoff, S., Hibberd, J. M., Nelson,
527 M. N., and Smith, S. A. 2015. Dissecting molecular evolution in the highly diverse plant
528 clade caryophyllales using transcriptome sequencing. *Molecular Biology and Evolution*,
529 32(8): 2001–2014.
- 530 Zhu, T., Dos Reis, M., and Yang, Z. 2015. Characterization of the uncertainty of
531 divergence time estimation under relaxed molecular clock models using multiple loci.
532 *Systematic Biology*, 64(2): 267–280.

Tables

Dataset	Orthologs	Clocklike (%)
BIR	7116	440 (6.18)
CAR	3767	274 (7.27)
CARY	583	3 (0.51)
HYM	1161	22 (1.89)
MIL	152	26 (17.10)
VIT	2267	8 (0.35)

Table 1: Dataset size and results of likelihood ratio tests for strict clock-like gene behavior.

Gene name	Variance	Tree length	Bipartition proportion
BIR			
12969	0.000791644	2.73068	0.5
1173	0.00205589	3.01712	0.457
12123	8.32228e-05	0.825943	0.413
CAR			
cluster259MIortho7	9.07832e-05	0.346618	1.0
cluster3790MIortho1	0.000245644	0.739886	1.0
cluster234MIortho1	0.0004849	1.19575	1.0
CARY			
cc7674-1-1to1ortho	0.0183029	10.9821	0.701
cc4427-1MIortho1	0.0093838	8.7827	0.657
cc7873-1MIortho1	0.0206222	10.4773	0.657
HYM			
cluster3024-1-1ortho1	0.00159156	2.64137	0.706
cluster5160-1-1ortho1	0.00294197	2.0815	0.706
cluster1251-1-1ortho1	0.00621115	4.99913	0.706
MIL			
cluster89-1-1ortho1	0.00200945	0.909593	0.875
cluster1437-1-1ortho1	0.00872612	2.96511	0.875
cluster1615-1-1ortho1	0.010942	3.56434	0.875
VIT			
cluster9579-1MIortho1	0.000978163	0.519373	1.0
cluster1236-1MIortho1	0.00106778	0.547562	1.0
cluster461-1MIortho1	0.001227	0.607536	1.0

Table 2: Properties of the genes used in the empirical dating analyses. Variance regards the root-to-tip paths. Tree length is measured in units of expected substitutions per site across all branches. Bipartition proportion measures agreement to the species tree topology (1.0 indicates complete concordance).

Dataset	Height	Lower	Higher
BIR	-0.26	0.27	-1.49
CAR	-0.004	0.04	-0.2
CARY	-3.93	0.52	-8.56
HYM	-0.12	0.1	-0.63
MIL	-0.09	0.04	-1.12
VIT	-0.02	0.08	-0.56

Table 3: The cumulative difference in the height, lower 95% HPD, and higher 95% HPD of each node comparing the UCLN estimates to the clock estimates from the individual empirical dating analyses. A value lower than 0 results when the cumulative difference in the clock values of height or HPD are younger than the associated UCLN values.

Dataset	Height		Lower		Higher		Nodes		Error	
	CL	UC	CL	UC	CL	UC	CL	UC	CL	UC
BIR	0.63	0.5	0.48	0.69	0.96	1.33	16	39	1.44	2.02
CAR	0.26	0.2	0.37	0.85	0.25	0.63	5	12	0.62	1.49
CARY	0.54	0.63	1.23	2.12	0.64	1.11	52	67	1.88	3.24
HYM	0.16	0.76	0.21	0.65	0.38	0.94	15	3	0.58	1.59
MIL	0.17	0.42	0.12	0.45	0.33	0.46	5	3	0.44	0.91
VIT	0.27	0.26	0.42	0.32	0.2	0.27	5	8	0.62	0.59

Table 4: Assessment of dating error for the clock (CL) and UCLN (UC) analyses of the simulated *clock* data. All measures involve distance from the true node age, and are cumulative sums across all nodes. Height is the inferred node age. Lower and Higher regard the 95% HPD node age bounds. Nodes indicates the number of true node ages contained within the HPD interval. Error is the total error involved, equivalent to Low + High.

Dataset	Height		Lower		Higher		Nodes		Error	
	CL	UC	CL	UC	CL	UC	CL	UC	CL	UC
BIR	1.26	3.21	1.26	6.43	1.37	1.52	12	24	2.64	7.95
CAR	0.76	0.69	0.89	1.59	0.68	0.58	2	9	1.57	2.17
CARY	2.29	3.51	2.37	8.98	2.38	4.97	15	55	4.75	13.95
HYM	0.14	0.91	0.61	3.01	0.61	1.58	18	16	1.22	4.65
MIL	0.14	0.61	0.32	1.6	0.57	1.17	11	10	0.89	2.77
VIT	0.29	1.12	0.82	2.43	0.29	0.73	14	9	1.11	3.16

Table 5: Assessment of dating error for the clock (CL) and UCLN (UC) analyses of the simulated *ucln* data. All measures involve distance from the true node age, and are cumulative sums across all nodes. Height is the inferred node age. Lower and Higher regard the 95% HPD node age bounds. Nodes indicates the number of true node ages contained within the HPD interval. Error is the total error involved, equivalent to Low + High.

534

Figures and Figure captions

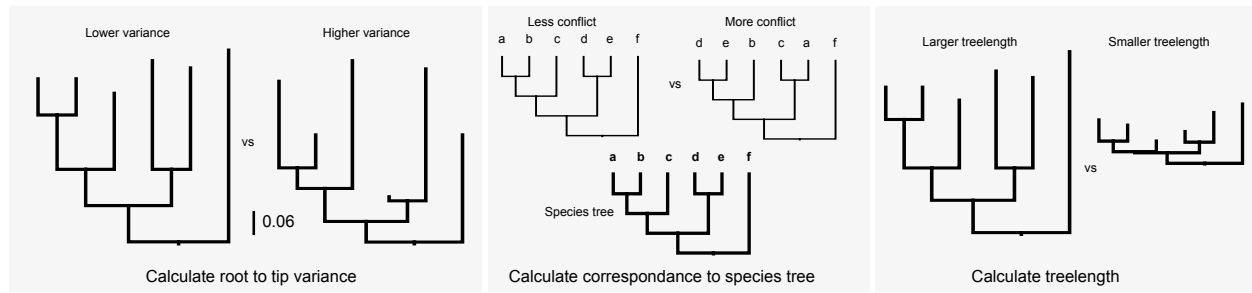


Figure 1: Measures used for sorting genes for use in dating analyses. The order presented here is arbitrary.

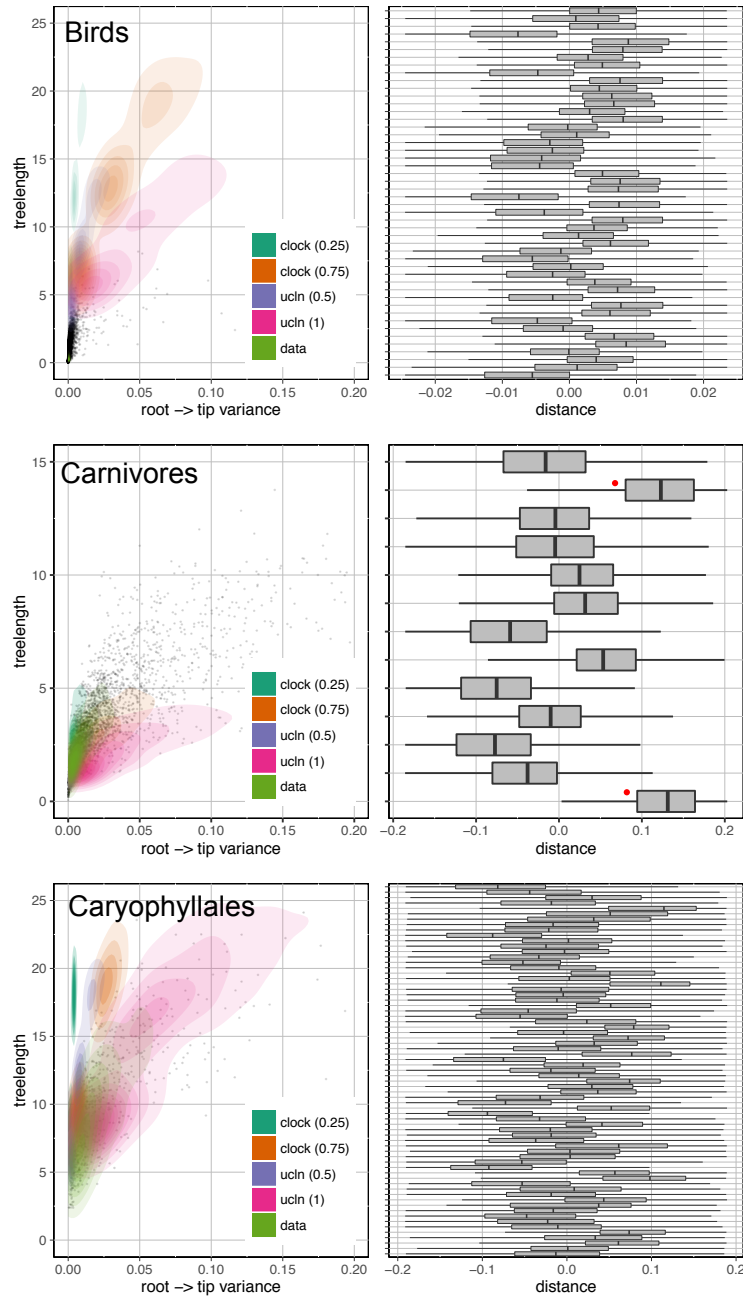


Figure 2: Plots of gene tree properties (left, including root-to-tip variance and treelength for simulated and empirical datasets) and tip-specific root-to-tip variance for empirical datasets (right). When the outgroup is present, the taxa are labeled with a red dot.

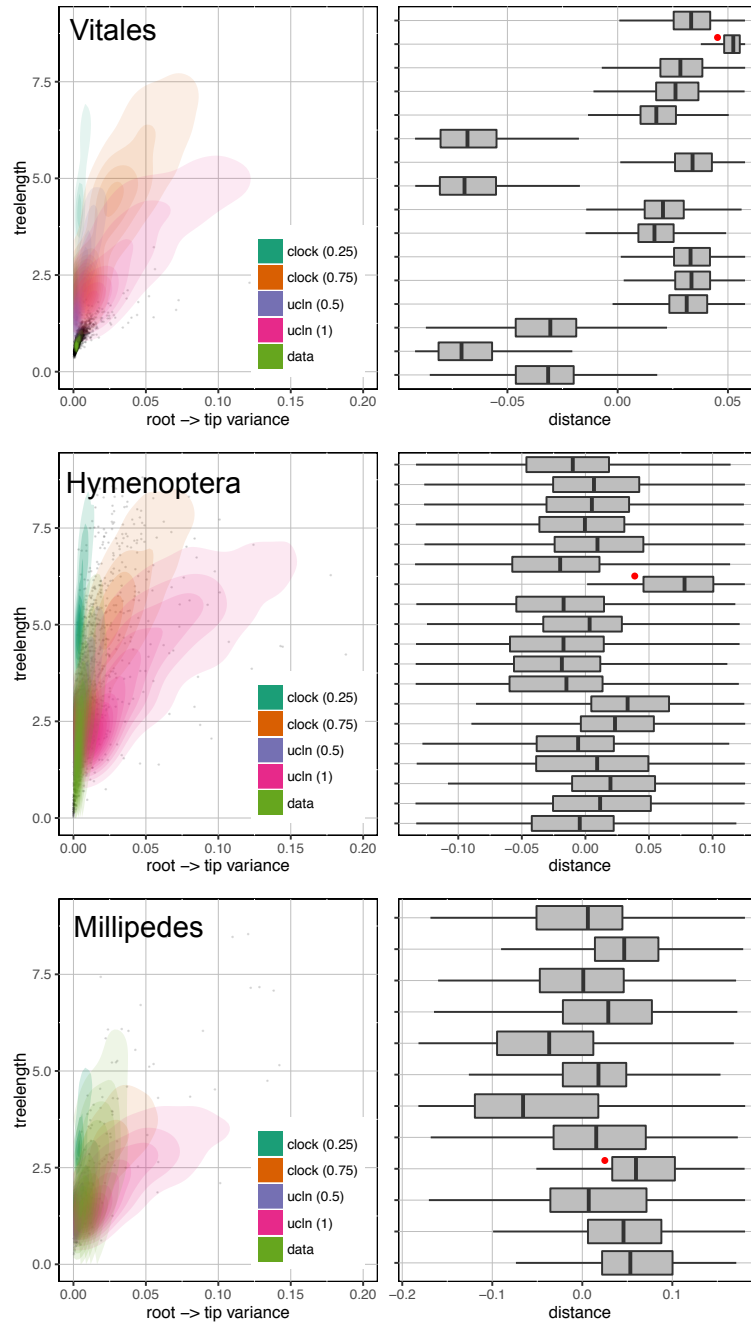


Figure 3: Plots of gene tree properties (left, including root-to-tip variance and treelength for simulated and empirical datasets) and tip-specific root-to-tip variance for empirical datasets (right). When the outgroup is present, the taxa are labeled with a red dot.

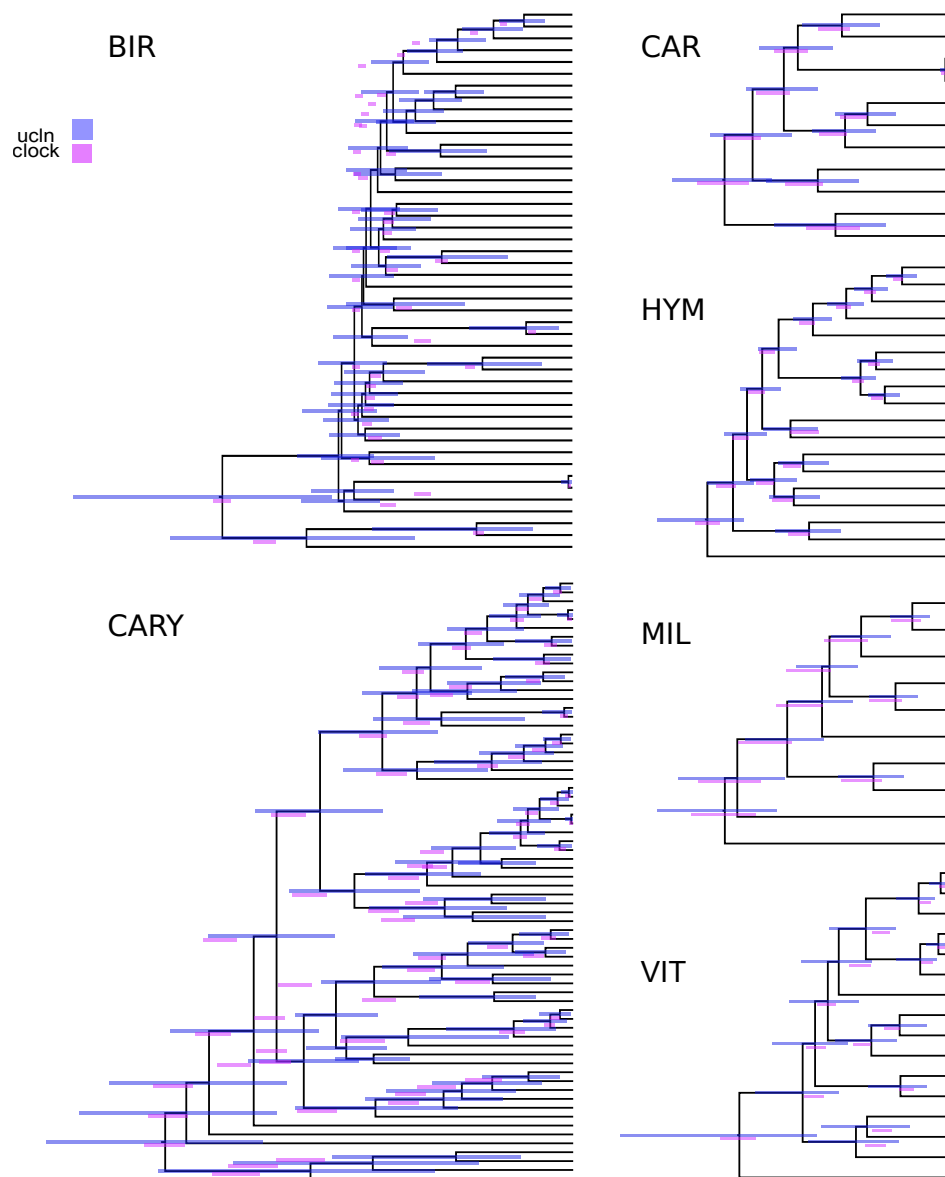


Figure 4: A comparison of strict clock and UCLN estimates of node ages for the six curated empirical datasets.

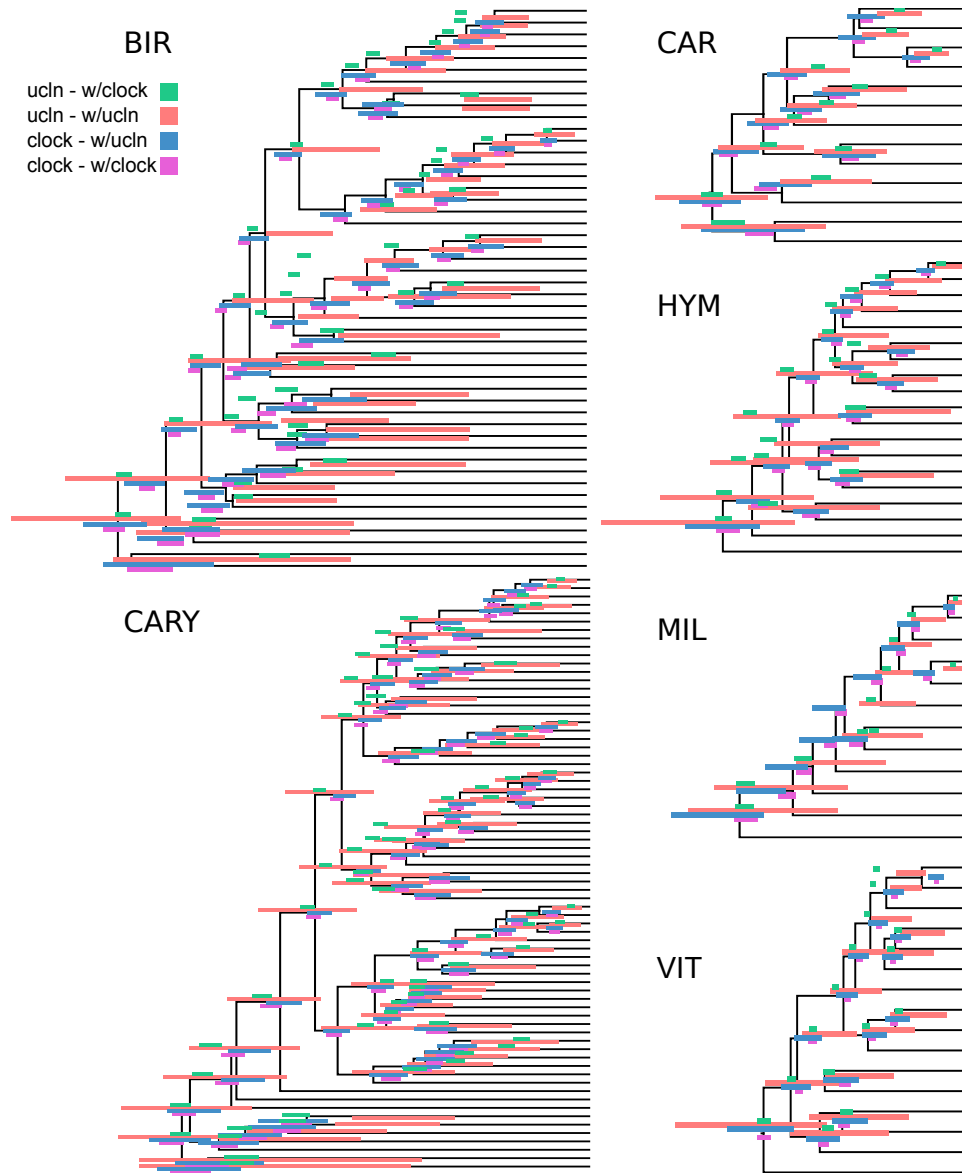


Figure 5: A comparison of strict clock and UCLN estimates of node ages for the simulated *clock* and *ucln* datasets. Red and pink are scenarios where the generating and inference are identical, while green and blue are where the models are mismatched.